

Aberystwyth University

Ice-rafted dropstones in 'post-glacial' Cryogenian cap carbonates

Le Heron, Daniel Paul; Busfield, Marie; Kettler, Christoph

Published in:

Geology

DOI:

[10.1130/G48208.1](https://doi.org/10.1130/G48208.1)

Publication date:

2020

Citation for published version (APA):

Le Heron, D. P., Busfield, M., & Kettler, C. (2020). Ice-rafted dropstones in 'post-glacial' Cryogenian cap carbonates. *Geology*, 49(3), 263-267. <https://doi.org/10.1130/G48208.1>

Document License

CC BY-NC

General rights

Copyright and moral rights for the publications made accessible in the Aberystwyth Research Portal (the Institutional Repository) are retained by the authors and/or other copyright owners and it is a condition of accessing publications that users recognise and abide by the legal requirements associated with these rights.

- Users may download and print one copy of any publication from the Aberystwyth Research Portal for the purpose of private study or research.
- You may not further distribute the material or use it for any profit-making activity or commercial gain
- You may freely distribute the URL identifying the publication in the Aberystwyth Research Portal

Take down policy

If you believe that this document breaches copyright please contact us providing details, and we will remove access to the work immediately and investigate your claim.

tel: +44 1970 62 2400

email: is@aber.ac.uk

1 Ice-rafted dropstones in 'post-glacial' Cryogenian cap 2 carbonates

3 Le Heron, D.P¹. Busfield, M.E²., Kettler, C¹.

4 ¹*Department of Geodynamics and Sedimentology, University of Vienna, Althanstrasse 14, 1090*

5 *Vienna, AUSTRIA. daniel.le-heron@univie.ac.at*

6 ²*Department of Geography and Earth Sciences, Aberystwyth University, Llandinam Building, Penglais*

7 *Campus, Aberystwyth, SY23 3DB.*

8

9 **Abstract**

10 Dropstones of ice-rafted origin are typically cited as key cold-climate evidence in Cryogenian strata,
11 and according to conventional wisdom should not occur in post-glacial, warm water carbonates. In
12 Namibia, the Chuos Formation (early Cryogenian) contains abundant dropstone-bearing intervals
13 and striated clasts. It is capped by the Rasthof Formation, comprising laminites in its lower portion,
14 and microbial carbonates above. These laminites are locally found to contain pebble- and granule-
15 sized lonestones in abundance. At Omutirapo (Fig. 1), metre-thick floatstone beds occur at the flanks
16 of a Chuos palaeovalley, and are readily interpreted as mass flow deposits. At Rasthof Farm,
17 however, the clasts warp, deflect and penetrate hundreds of carbonate laminations at both the
18 outcrop and thin section scale. We propose that these are dropstones, and envisage an ice-rafting
19 mechanism. Evidence for vestigial glaciation concomitant with cap carbonate deposition thus merits
20 a reappraisal of the depositional conditions of cap carbonates and their palaeoclimatic significance.

21

22

23 INTRODUCTION

24 The glacial affinity of diamictites and lonestone-bearing sedimentary rocks in the Cryogenian record
25 is compelling (Hoffman and Halverson, 2008; Le Heron et al., 2013; Busfield et al., 2013; Bechstädt et
26 al., 2018; Hoffman et al., 2017). By comparison, all models for cap carbonates envisage a postglacial
27 origin (Yu et al., 2020). These are commonly thought to record a high alkalinity flux and sudden
28 oceanic oxidation following rapid meltback of global ice cover (e.g. Shields, 2005; Hoffman et al.,
29 1998), possibly representing stratigraphic condensation during globally synchronous deglaciation
30 (Rooney et al., 2020).

31 In Namibia, the Chuos Formation (of glacial origin) is overlain by the Rasthof Formation (cap
32 carbonate) that is interpreted to record the abrupt change to a significantly warmer greenhouse
33 climate (Hoffmann and Prave, 2004; Hoffman et al., 2017). Here, we compare evidence from two
34 outcrops of the Rasthof Formation, both of which contain clast-rich intervals sandwiched between
35 clast-free dololaminites. One of these (from Omutirapo) represents a mass flow deposit; another
36 from Rasthof Farm, with lonestones puncturing delicate laminites, is interpreted as a cluster of ice-
37 rafted dropstones. We posit that the dropstones require the presence of floating ice to explain their
38 occurrence in the purportedly warm water cap carbonates, with implications for Cryogenian
39 deglaciation on a global-scale.

40

41 GEOLOGIC BACKGROUND AND STUDY AREA

42 Cryogenian glacial (diamictite-bearing siliciclastics) and postglacial (cap carbonate) rocks crop out
43 along the southern and western flanks of the Owambo Basin, northern Namibia (**Fig. 1**) (Miller,
44 2008). Diamictite-bearing rocks of the Chuos Formation sit unconformably upon the Nosib
45 Sandstone Group, with the Rasthof Formation in turn lying above (**Fig. 2**). At Omutirapo (**Fig. 1**), the
46 Chuos Formation attains >400 m thickness in a glacial palaeovalley and is interbedded with

47 lonestone-bearing and lonestone-free intervals (Le Heron et al., 2013), which record glacial to
48 interglacial transitions. Subsequent work (Hoffman et al., 2017) at Omutirapo has confirmed earlier
49 interpretations of a major subglacial topography. Detailed micromorphological studies have
50 distinguished glacial from non-glacial modes of emplacement for diamictites by comparison to
51 modern and Quaternary subglacial diamicts (Busfield et al., 2013; Busfield and Le Heron, 2018). The
52 role of mass flow sedimentation in the Chuos (Eyles and Januszczak, 2007) remains undisputed
53 although the evidence for glacial processes also remains strong (Le Heron et al., 2013). The Rasthof
54 Formation is a cap carbonate that directly overlies the Chuos (Hoffman and Halverson, 2008), and
55 which comprises a micritic dololaminite member overlain by a microbial member comprising
56 stromatolites and thrombolites (Le Ber et al., 2013). A marine origin is suggested on account of the
57 agglutinated foraminifera that it contains (e.g. Bosak et al., 2012, Dalton et al., 2013). In
58 palaeogeographic terms, the study areas represent rocks deposited on a stable marine platform (the
59 Northern Platform: Hoffman et al., 2008). A second diamictite-rich interval, the Ghaub Formation,
60 occurs at a higher level in the stratigraphy. Bechstädt et al. (2018) noted that a non-glacial origin for
61 the diamictites “is questioned by possible dropstones that occur in beds transitional to and, rarely,
62 also within the cap carbonates”. Thus, the occurrence of “possible dropstones” in other cap
63 carbonate successions, such as the Rasthof Formation, merits reappraisal.

64

65 **DESCRIPTION**

66 We studied two exposures in which outsized clasts (lonestones) occur within the Rasthof Formation.
67 These are (i) the Omutirapo succession and (ii) at Rasthof Farm (**Fig. 1**). In both cases, the uppermost
68 part of the Chuos Formation comprises massive diamictite, and the basal part of the Rasthof
69 Formation comprises delicately laminated dolomicrites which sit in sharp contact upon the
70 underlying glacial deposits (**Fig. 2, Fig. 3 A**). Lonestone-bearing carbonates (granule to pebble-sized
71 clasts embedded in a micrite matrix) are common. Two subfacies are recognised. First, at

72 Omutirapo, ca. 10 m thick laminated dolomicrites contain a 1 m thick floatstone bed (**Fig. 3 B**) which
73 passes along strike over ca. 100 m into normally-graded packstones (**Fig. 3 C**). The floatstone interval
74 contains sub-rounded to rounded, equant, dolostone clasts (**Fig. 3 D**), with highly attenuated,
75 bedding parallel clasts in the basal 10 cm (**Fig. 3 E**). Second, at Rasthof Farm (**Fig. 2, Fig. 4 A**), a 50 cm
76 interval of mm-thick laminated dolomicrites, contains abundant granule to small pebble-sized
77 lonestones up to 2 cm diameter (**Fig. 4 B**). At the outcrop / hand-specimen scale, lonestone-bearing
78 laminations are sandwiched between dololaminites in which outsized clasts are absent (**Fig. 4 B**).
79 Most lonestones exhibit both impact structures beneath them, and draping lamination (undisturbed
80 dololaminae) overlie them (Fig. 4 B-E). Small, lens-like clast clusters (**Fig. 4 B**) also occur. Clasts
81 include abundant dolomite granules, quartz (**Fig. 4 C, D**) and lithic fragments (**Fig. 4 E**). At the thin-
82 section scale, the occurrence of lonestones at multiple levels is demonstrable (**Fig. 4 F**). Both
83 irregular clast clusters and individual clasts, including 1 cm diameter intraclasts (**Fig. 4 F**) punctuate
84 mm-thick laminae, and are draped by undisturbed dolomicrite laminae. A full 3D model of the
85 sampled interval is available as Supplementary Material.

86

87 **INTERPRETATION**

88 The lonestone-bearing carbonates at Omutirapo and Rasthof Farm are attributable to two different
89 processes. At Omutirapo, the absence of laminations (**Fig. 3 C**) is compatible with gravitational
90 emplacement as previously suggested (Hoffman et al., 2008), in which attenuated basal clasts (**Fig. 3**
91 **E**) probably record shearing at the base of a mass flow. Cap carbonate collapse facies are now widely
92 recognised elsewhere (e.g. Creveling et al., 2016), and at Omutirapo, a non-glacial mechanism is
93 envisaged. At Rasthof Farm, by contrast, we propose that the lonestone-bearing laminite interval
94 records ice-rafted deposition. Puncturing of mm-thick laminae by granule- to pebble-sized clasts
95 testifies to their emplacement from above, representing settling through a water column. They are
96 thus interpreted as ice rafted debris (IRD). Their presence within finely laminated dolomicrites is

97 thus hydrodynamically paradoxical (Bennett et al., 1996). The clast clusters are interpreted as
98 sedimentary pellets (Tomkins et al., 2008). Although there is a tradition of recognising “outrunner
99 clasts” from debris flows where an ice-rafted mechanism is not appealing (Kennedy and Eyles, 2020),
100 this process cannot explain granule and pebble-sized clasts in laminated dolomicrites. This is because
101 although hydroplaning beneath much larger-scale “outrunner blocks” e.g. in olistostromes is
102 possible, the mechanics do not work at the finer-grained end of the Udden-Wentworth scale (Peakall
103 et al., 2020). Furthermore, the absence in the study interval of wave-ripple (Lamb et al., 2012) or
104 hummocky cross stratification structures locally seen elsewhere in the Rasthof (Le Ber et al., 2013)
105 rules out a tractive origin for the lonestones.

106 In the Paleozoic record, kelp or fucid rafting explains some dropstones (Zalasiewicz and
107 Taylor, 2001). Time-calibrated phylogeny of green seaweeds (Del Cortona et al., 2020) suggests that
108 their ancestors may have been present in the Cryogenian. Yet rafting by seaweeds torn from the
109 shore (e.g. by storms) is incompatible with interpretations of the dololaminites in the Rasthof. These,
110 like other dololaminites in cap carbonates record pelagic precipitation, irrespective whether this is
111 chemically or biogenically mediated (c.f. Hoffman and Schrag, 2002; Shields, 2005; Kennedy and
112 Christie-Blick, 2011). Thus, given the absence of other mechanisms which could adequately explain
113 the emplacement of dropstones (seaweed rafting, driftwood rafting, gastroliths: Bennett et al.,
114 1996) we find that they indicate floating ice during Rasthof deposition. This finding is significant,
115 because “no convincing dropstone has been confirmed from cap dolostone units anywhere in the
116 world” (Shields, 2005, p.301).

117

118

119

120

121 **DISCUSSION AND CONCLUSIONS**

122 Two scenarios for the IRD emerge: (i) as glacial sediment advected into open water by either an ice
123 shelf or calving icebergs, or alternatively (ii) through melting sea ice. Additional physical evidence for
124 iceberg activity (e.g. iceberg keel plough marks: Vesely and Assine, 2014) has never been found in
125 the Cryogenian record. Analysis of cores through Heinrich layers in the polar North Atlantic reveals
126 IRD are up to small pebble-size and concentrated along discrete horizons and linked to major iceberg
127 calving events (Hodell et al., 2017). In contrast, the Rasthof Farm IRD are scattered over hundreds of
128 laminations, suggesting multiple ice melting events.

129 The development of floating sea ice or ice shelves must therefore be considered. Pebble-
130 sized clasts, deposited through shorefast ice in large lakes can also occur (Oviatt, 2018), and thus
131 clast size is of little use in inferring the nature of the floating ice source. In modern high latitude
132 settings such as the Antarctic Peninsula, eolian sediment is transported over seasonal sea ice during
133 the winter months. Upon melting, sand particles are released into the open marine environment
134 (Chewings et al., 2014). These processes result in dispersed sand and granule sized particles in
135 laminites. The same processes explain a significant component of open marine sedimentation in the
136 Arctic, whereby the advection of sand and coarser material over developing frazil ice, together with
137 mud-grade sediment, is also well established (Kempena et al., 1989). Basal meltout beneath floating
138 ice shelves would also account for IRD, in which the sedimentary pellets may be interpreted as
139 meltout of till (Tomkins et al., 2008).

140 In terms of the host strata, dololaminites above Cryogenian glacial successions are classically
141 considered to result from a massive alkalinity flux stimulated through either carbon dioxide
142 (Hoffman et al., 1998) or methane (Kennedy et al., 2001) outgassing, through continental
143 weathering of freshly exposed continental material (Hoffman et al., 2017), or by the precipitation of
144 whittings during algal blooms within a low salinity meltwater plume (Shields, 2005). Some have
145 proposed that tillite weathering might account for cap carbonate deposition (Fabre and Berger,

146 2012). This latter mechanism has parallels with the proposals of Fairchild et al. (1989) who suggested
147 that “massive recrystallization of glacially transported carbonate is proposed as a geologically
148 significant process”. All of these mechanisms require that the dololaminites represent pelagic
149 materials deposited postglacially in an ameliorated climate. Assuming a global ice cover, energy-
150 balance calculations have suggested a global mean surface temperature swing from -50 C during a
151 glaciation to approximately +40 C during interglacial (cap carbonate) times (Hoffman and Schrag,
152 2002, their Fig. 7). Such high temperatures are difficult to reconcile with the scattered occurrence of
153 the dropstones across hundreds of laminae: a sudden melting mechanism would instead be
154 expected to release an iceberg armada and intense concentration of dropstones across a single
155 stratigraphic interval. These textures are not observed at Rasthof Farm.

156 As precedents, dropstones are now recognised to occur in other Neoproterozoic successions
157 where according to conventional wisdom they should not occur, such as ca. 1000 Ma (Tonian) ice
158 rafted debris in Scotland (Hartley et al., 2020). In south China, presence of dropstones in the
159 Doushanto Formation cap carbonate has been suggested but not fully described (Huang et al., 2016).
160 Cap carbonate dololaminite facies are often viewed as condensed sedimentation deposits (Kennedy
161 and Christie-Blick, 2011; Rooney et al., 2020). In the Amadeus Basin, Australia, they may represent
162 basinal facies which by comparison to other cap dolostones may represent tens of millions of years
163 (Kennedy and Christie-Blick, 2011). Whilst rates of deposition of the cap dolostones are unknown,
164 consideration of Cryogenian glacial successions that underlie such sequences point to extremely low
165 rates of accumulation by comparison to Phanerozoic glaciations (Partin and Sadler, 2016), which
166 would also be consistent with a “condensed” origin for the glacial facies (Kennedy and Christie-Blick,
167 2011). If the Rasthof dololaminites do represent many millions of years deposition, then they testify
168 to the operation of ice-rafting processes over a similar time interval.

169 The juxtaposition of what have traditionally been regarded as warm water cap carbonates
170 immediately overlying cold climate diamictites is an intriguing paradox of the Cryogenian icehouse.

171 The boundary between the two has been recognised and correlated worldwide and used to attest to
172 globally synchronous terminal deglaciation at least twice during the Neoproterozoic, with cap
173 carbonates viewed as isochronous (e.g. Rooney et al., 2020; Yu et al., 2020). The presence of
174 recurring dropstone horizons in one of the iconic cap carbonates casts suggests that existing models
175 must be reappraised to incorporate the presence of ice during deposition. It further questions the
176 chronostratigraphic significance of these deposits as the definitive marker of the end of Cryogenian
177 glaciation in one locality, inviting a careful reconsideration of their significance on a global scale.

178

179 **Acknowledgments**

180 We are grateful to Max Lechte, to two anonymous reviewers, and the input of the editor William
181 Clyde whose suggestions on an earlier version of the paper improved the manuscript greatly.

182

183 **REFERENCES CITED**

- 184 Bechstädt, T., Jäger, H., Rittersbacher, A., Schweisfurth, B., Spence, G., Werner, G., and Boni, M.,
185 2018, The Cryogenian Ghaub Formation of Namibia – New insights into Neoproterozoic glaciations:
186 *Earth-Science Reviews*, v. 177, p. 678–714. <https://doi.org/10.1016/j.earscirev.2017.11.028>
- 187 Bennett, M. R., Doyle, P., and Mather, A. E., 1996, Dropstones: Their origin and significance:
188 *Palaeogeography, Palaeoclimatology, Palaeoecology*, v. 121, p. 331–339.
189 [https://doi.org/10.1016/0031-0182\(95\)00071-2](https://doi.org/10.1016/0031-0182(95)00071-2)
- 190 Bosak, T., Lahr, J.G., Pruss, S.B., MacDonald, F.A., Gooday, A.J., Dalton, L., and Matys, E.D., 2012,
191 Possible early foraminiferans in post-Sturtian (713–636 Ma) cap carbonates: *Geology*, v. 40, p. 67–
192 70.
- 193 Busfield, M. E., and Le Heron, D. P., 2013, Glacitectonic deformation in the Chuos formation of
194 northern Namibia: Implications for Neoproterozoic ice dynamics: *Proceedings of the Geologists’*
195 *Association*, v. 124. <https://doi.org/10.1016/j.pgeola.2012.10.005>
- 196 Busfield, M. E., and Le Heron, D. P., 2018, Snowball earth under the microscope: *Journal of*
197 *Sedimentary Research*, v. 88. <https://doi.org/10.2110/jsr.2018.34>

198 Chewings, J. M., Atkins, C. B., Dunbar, G. B., and Golledge, N. R., 2014, Aeolian sediment transport
199 and deposition in a modern high-latitude glacial marine environment: *Sedimentology*, 61, p. 1535–
200 1557. <https://doi.org/10.1111/sed.12108>

201 Dalton, L.A., Bosak, T., Macdonald, F.A., Lahr, D.J.G., and Pruss, S.B., 2013, Preservation and
202 morphological variability of assemblages of agglutinated eukaryotes in Cryogenian cap carbonates of
203 northern Namibia: *Palaios*, v. 28, p. 67–79.

204 Del Cortona, A., Jackson, C. J., Bucchini, F., Van Bel, M., D’hondt, S., Skaloud, P., Delwiche, C. F.,
205 Knoll, A. H., Raven, J. A., Verbruggen, H., Vandepoele, K., De Clerck, O., and Leliaert, F., 2020,
206 Neoproterozoic origin and multiple transitions to macroscopic growth in green seaweeds:
207 *Proceedings of the National Academy of Sciences of the United States of America*, v. 117, p. 2551–
208 2559. <https://doi.org/10.1073/pnas.1910060117>

209 Eyles, N. and Januszczak, N., 2007, Syntectonic subaqueous mass flows of the Neoproterozoic Otavi
210 Group, Namibia: where is the evidence of global glaciation? *Basin Research*, v. 19, p. 179–198.

211 Fabre, S., and Berger, G., 2012, How tillite weathering during the snowball Earth aftermath induced
212 cap carbonate deposition: *Geology*, v. 40, p. 1027–1030. <https://doi.org/10.1130/G33340.1>

213 Fairchild, I.J., Hambrey, M.J., Spiro, B., and Jefferson, T.H., 1989, Late Proterozoic glacial carbonates
214 in northeast Spitsbergen: new insights into the carbonate-tillite association: *Geological Magazine*, v.
215 126, p. 469-490.

216 Hartley, A., Kurjanski, B., Pugsley, J., and Armstrong, J., 2019, Ice-rafting in lakes in the early
217 Neoproterozoic: dropstones in the Diabaig Formation, Torridon Group, NW Scotland: *Scottish
218 Journal of Geology*, <https://doi.org/10.1144/sjg2019-017>

219 Hodell, D. A., Nicholl, J. A., Bontognali, T. R. R., Danino, S., Dorador, J., Dowdeswell, J. A., Einsle, J.,
220 Kuhlmann, H., Martrat, B., Mleneck-Vautravers, M. J., Rodríguez-Tovar, F. J., and Röhl, U., 2017,
221 Anatomy of Heinrich Layer 1 and its role in the last deglaciation: *Paleoceanography*, v. 32, p. 284–
222 303. <https://doi.org/10.1002/2016PA003028>

223 Hoffman, P. F., and Schrag, D. P., 2002, The snowball Earth hypothesis: Testing the limits of global
224 change: *Terra Nova*, v. 14, p. 129–155. <https://doi.org/10.1046/j.1365-3121.2002.00408.x>

225 Hoffman, P.F. and Halverson, G.P., 2008, Otavi Group of the western Northern Platform, the eastern
226 Kaoko Zone and the western Northern Margin Zone: In: *The Geology of Namibia Volume 2 –
227 Neoproterozoic to Lower Palaeozoic* (Ed. R. McG Miller), pp. 13.69–13.136. Ministry of Mines and
228 Energy, Windhoek, Namibia.

229 Hoffman, P. F., Kaufman, A. J., Halverson, G. P., and Schrag, D. P., 1998, A Neoproterozoic snowball
230 Earth: *Science*, v. 281, p. 1–5. <https://doi.org/10.1126/science.281.5381.1342>

231 Hoffman, P. F., Lamothe, K. G., LoBianco, S. J. C., Hodgskiss, M. S. W., Bellefroid, E. J., Johnson, B. W.,
232 Hodgkin, E. B., and Halverson, G. P., 2017, Sedimentary depocenters on Snowball Earth: Case studies
233 from the Sturtian Chuos formation in Northern Namibia: *Geosphere*, v. 13, p. 811–837.
234 <https://doi.org/10.1130/GES01457.1>

235 Huang, K. J., Teng, F. Z., Shen, B., Xiao, S., Lang, X., Ma, H. R., Fu, Y., and Peng, Y., 2016, Episode of
236 intense chemical weathering during the termination of the 635 Ma Marinoan glaciation: Proceedings
237 of the National Academy of Sciences of the United States of America, v. 113, p. 14904–14909.
238 <https://doi.org/10.1073/pnas.1607712113>

239 Kennedy, K. and Eyles, N., 2020, Syn-rift mass flow generated ‘tectonofacies’ and ‘tectonosequences’
240 of the Kingston Peak Formation, Death Valley, California, and their bearing on supposed
241 Neoproterozoic panglacial climates: Sedimentology, <https://doi.org/10.1111/sed.12781>

242 Kennedy, M. J., and Christie-Blick, N., 2011, Condensation origin for Neoproterozoic cap carbonates
243 during deglaciation: Geology, v. 39, p. 319–322. <https://doi.org/10.1130/G31348.1>

244 Kennedy, M. J., Christie-Blick, N., and Sohl, L. E., 2001, Are Proterozoic cap carbonates and isotopic
245 excursions a record of gas hydrate destabilization following Earth’s coldest intervals? Geology, v. 29,
246 p. 443–446. [https://doi.org/10.1130/0091-7613\(2001\)029<0443:APCCAI>2.0.CO;2](https://doi.org/10.1130/0091-7613(2001)029<0443:APCCAI>2.0.CO;2)

247 Lamb, M. P., Fischer, W. W., Raub, T. D., Taylor Perron, J., and Myrow, P. M., 2012, Origin of giant
248 wave ripples in snowball earth cap carbonate: Geology, v. 40, p. 827–830.
249 <https://doi.org/10.1130/G33093.1>

250 Le Ber, E., Le Heron, D. P., Winterleitner, G., Bosence, D. W. J., Vining, B. A., and Kamona, F., 2013,
251 Microbialite recovery in the aftermath of the Sturtian glaciation: Insights from the Rasthof
252 Formation, Namibia: Sedimentary Geology, v. 294, p. 1–12.
253 <https://doi.org/10.1016/j.sedgeo.2013.05.003>

254 Le Heron, D. P., Busfield, M. E., and Kamona, F., 2013, An interglacial on snowball Earth? Dynamic ice
255 behaviour revealed in the Chuos Formation, Namibia: Sedimentology, v. 60, p. 411–427.
256 <https://doi.org/10.1111/j.1365-3091.2012.01346.x>

257 Oviatt, C. G. J., 2019, Geomorphic controls on sedimentation in Pleistocene Lake Bonneville, eastern
258 Great Basin. From Saline to Freshwater: The Diversity of Western Lakes in Space and Time, 2536(04),
259 53–66. [https://doi.org/10.1130/2018.2536\(04\)](https://doi.org/10.1130/2018.2536(04))

260 Partin, C.A., and Sadler, P.M., 2016, Slow net sediment accumulation sets snowball Earth apart from
261 all younger glacial episodes: Geology 44, 1019-1022.

262 Peakall, J., Best, J., Baas, J.H., Hodgson, D.M., Clare, M.A., Talling, P.J., Dorrell, R.M., Lee, D.R., 2020,
263 An integrated process-based model of flutes and tool marks in deep-water environments:
264 Implications for palaeohydraulics, the Bouma sequence and hybrid event beds: Sedimentology, v. 67,
265 p. 1601–1666. <https://doi.org/10.1111/sed.12727>

266 Rodríguez-López, J. P., Liesa, C. L., Pardo, G., Meléndez, N., Soria, A. R., and Skilling, I., 2016, Glacial
267 dropstones in the western Tethys during the late Aptian-early Albian cold snap: Palaeoclimate and
268 palaeogeographic implications for the mid-Cretaceous. Palaeogeography, Palaeoclimatology,
269 Palaeoecology: v. 452, p. 11–27. <https://doi.org/10.1016/j.palaeo.2016.04.004>

270 Rooney, A.D., Yang, C., Condon, D.J., Zhu, M., Macdonald, F.A., 2020, U-Pb and Re-Os geochronology
271 tracks stratigraphic condensation in the Sturtian snowball Earth aftermath: Geology, v. 48, p. 625–
272 629. <https://doi.org/10.1130/G47246.1>

- 273 Shields, G. A., 2005, Neoproterozoic cap carbonates: A critical appraisal of existing models and the
 274 plumeworld hypothesis: *Terra Nova*, v. 17, p. 299–310. [https://doi.org/10.1111/j.1365-](https://doi.org/10.1111/j.1365-3121.2005.00638.x)
 275 [3121.2005.00638.x](https://doi.org/10.1111/j.1365-3121.2005.00638.x)
- 276 Tomkins, J.D., Lamoureux, S.F., Antoniadou, D., Vincent, W.F., 2008, Sedimentary pellets as an ice-
 277 cover proxy in a High Arctic ice-covered lake: *Journal of Paleolimnology*, v. 41, p. 225-242.
 278 <https://doi.org/10.1007/s10933-008-9255-x>
- 279 Vesely, F. F., and Assine, M. L., 2014, Ice-Keel Scour Marks In the Geological Record: Evidence From
 280 Carboniferous Soft-Sediment Striated Surfaces In the Parana Basin, Southern Brazil: *Journal of*
 281 *Sedimentary Research*, v. 84, p. 26–39. <https://doi.org/10.2110/jsr.2014.4>
- 282 Yan, B., Shen, W., Zhao, N., and Zhu, X., 2020, Constraints on the nature of the Marinoan glaciation:
 283 Cyclic sedimentary records from the Nantuo Formation, South China: *Journal of Asian Earth Sciences*,
 284 v. 189, 104137. <https://doi.org/10.1016/j.jseaes.2019.104137>
- 285 Yu, W., Algeo, T.J., Zhou, Q., Du, Y., Wang, P. 2020. Cryogenian cap carbonate models: a review and
 286 critical assessment. *Palaeogeography, Palaeoclimatology, Palaeoecology*, 552, 109727.
- 287 Zalasiewicz, J., and Taylor, L., 2001, Deep-basin dropstones in the early Silurian of Wales: A clue to
 288 penecontemporaneous, near-shore algal forests: *Proceedings of the Geologists' Association*, v. 112,
 289 p. 63–66. [https://doi.org/10.1016/S0016-7878\(01\)80050-X](https://doi.org/10.1016/S0016-7878(01)80050-X)

290

291

292 **Figure captions**

293 *Figure 1:* Geotectonic map of northern Namibia (after Hoffman and Halverson, 2008), showing the
 294 location of the two study areas at Omutirapo (19° 6.999'S, 13° 56.170'E) and Rasthof Farm (19°
 295 20.004'S, 14° 44.272'E).

296 *Figure 2:* A. Stratigraphy of the Otavi Group. The maximum age constraint for the Chuos, 747 ± 2 Ma,
 297 is based on U-Pb dating of Askevold Formation volcanics in the Ombombo Subgroup (Hoffmann et
 298 al., 2004). The upper glacial unit, the Ghaub, exhibits a 635 ± 1 Ma depositional age from U-Pb dating
 299 of ash beds (Hoffman et al., 1996). B: Summary sedimentary logs of the uppermost part of the Chuos
 300 Formation (base not shown) and the lower part of the Rasthof Formation at both Omutirapo and
 301 Rasthof Farm.

302 *Figure 3:* Stratigraphic relationships and lonestone-bearing strata at Omutirapo. A: Stratigraphic
 303 contact between sheared diamictites of the Chuos Formation (below the hammer) and dololaminites
 304 of the basal Rasthof Formation (above the hammer). B: a tripartite interval consisting of
 305 dololaminites at the base, normally graded packstone-grainstone in the middle, and dololaminites at
 306 the top. C: ca. 1 m thick floatstone interval sandwiched between dololaminites. This floatstone
 307 interval is the lateral equivalent of the normally graded packstone-grainstone shown in B. D: Detail
 308 of the floatstone bed with sub-rounded to rounded clasts. E: Sheared and attenuated clasts at the
 309 bottom of the floatstone interval in C (next to the head of the hammer).

310 *Figure 4:* Outcrop view of the section at Rasthof Farm, showing vertically inclined strata that young
311 to the left. The position of the profile in Fig. 2 is shown, as it the location of the lonestone-bearing
312 strata in the Rasthof Formation. A: Dololaminites with abundant lonestones, many of which show
313 evidence for impact structures, punctured underlying laminations and undisturbed, draping
314 laminations. Note also the presence of a “clast cluster” at the bottom right hand corner of the
315 image. Evidence for normal faults with mm-scale offset, capped by undisturbed laminations, is seen
316 throughout the section. C and D: Quartz granule in disturbed laminations; note also the presence of
317 pyrite (Pyr) throughout. E: Two examples of completely isolated lonestones within the dololaminites,
318 each showing impact structures. F: Thin section image. Upper part is largely undeformed, with
319 evidence for impact structures beneath lonestones and undisturbed, draping laminations. The
320 bottom part of the image shows multiple lines of evidence for soft-sediment deformation, including
321 a normal fault and intralamina folds. These features are interpreted as the products of early
322 compaction.

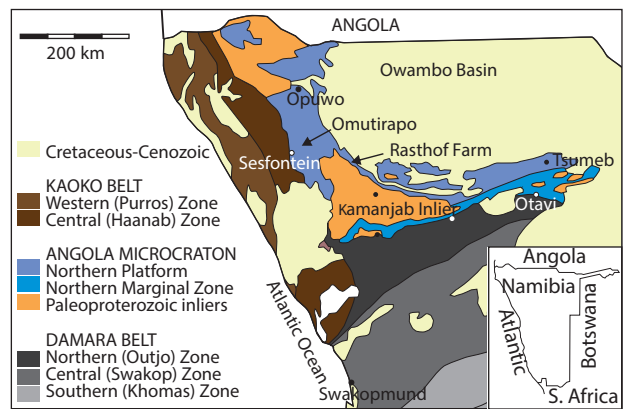
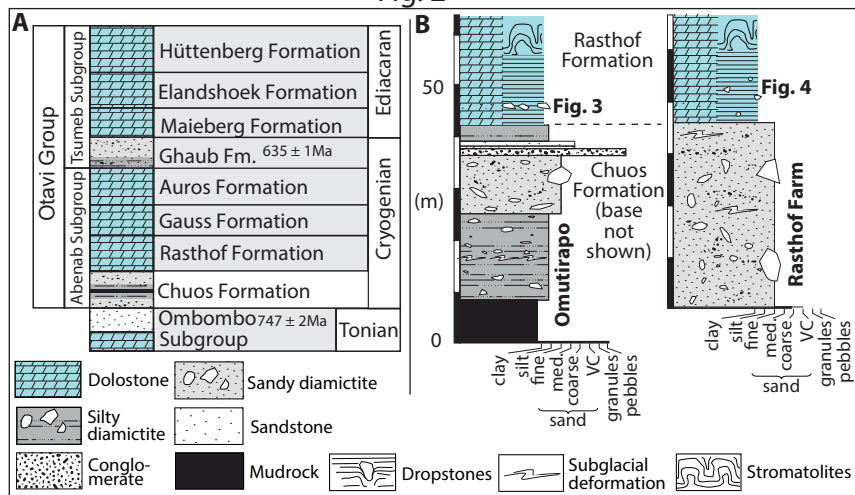


Fig. 1

Fig. 2



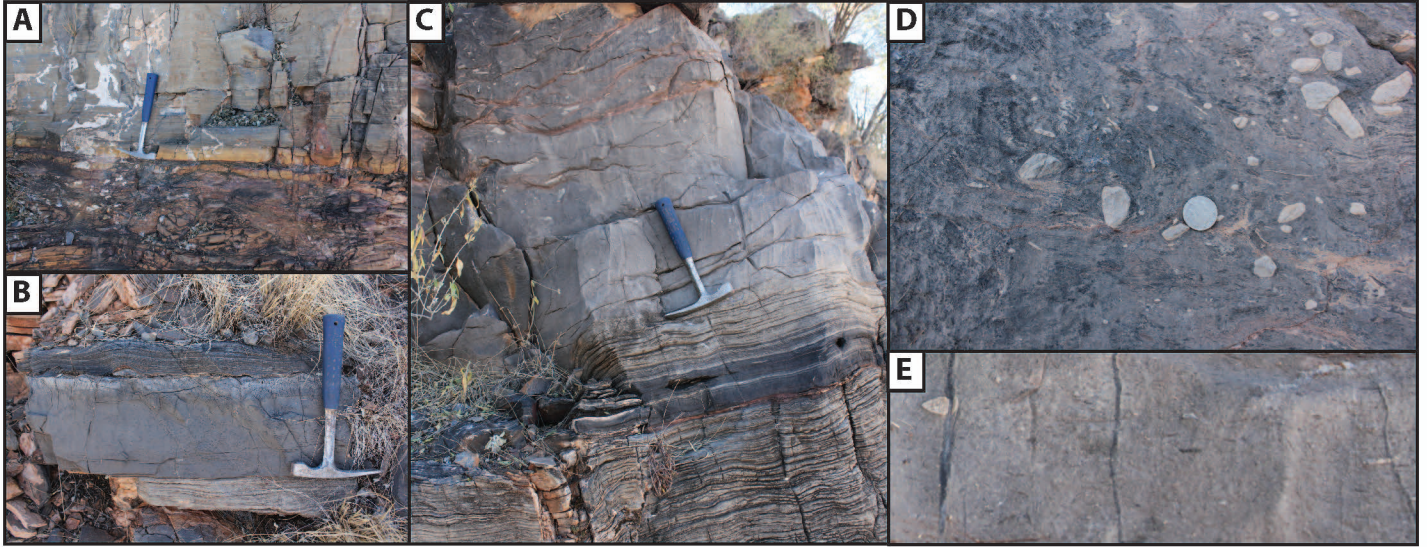


Fig. 3

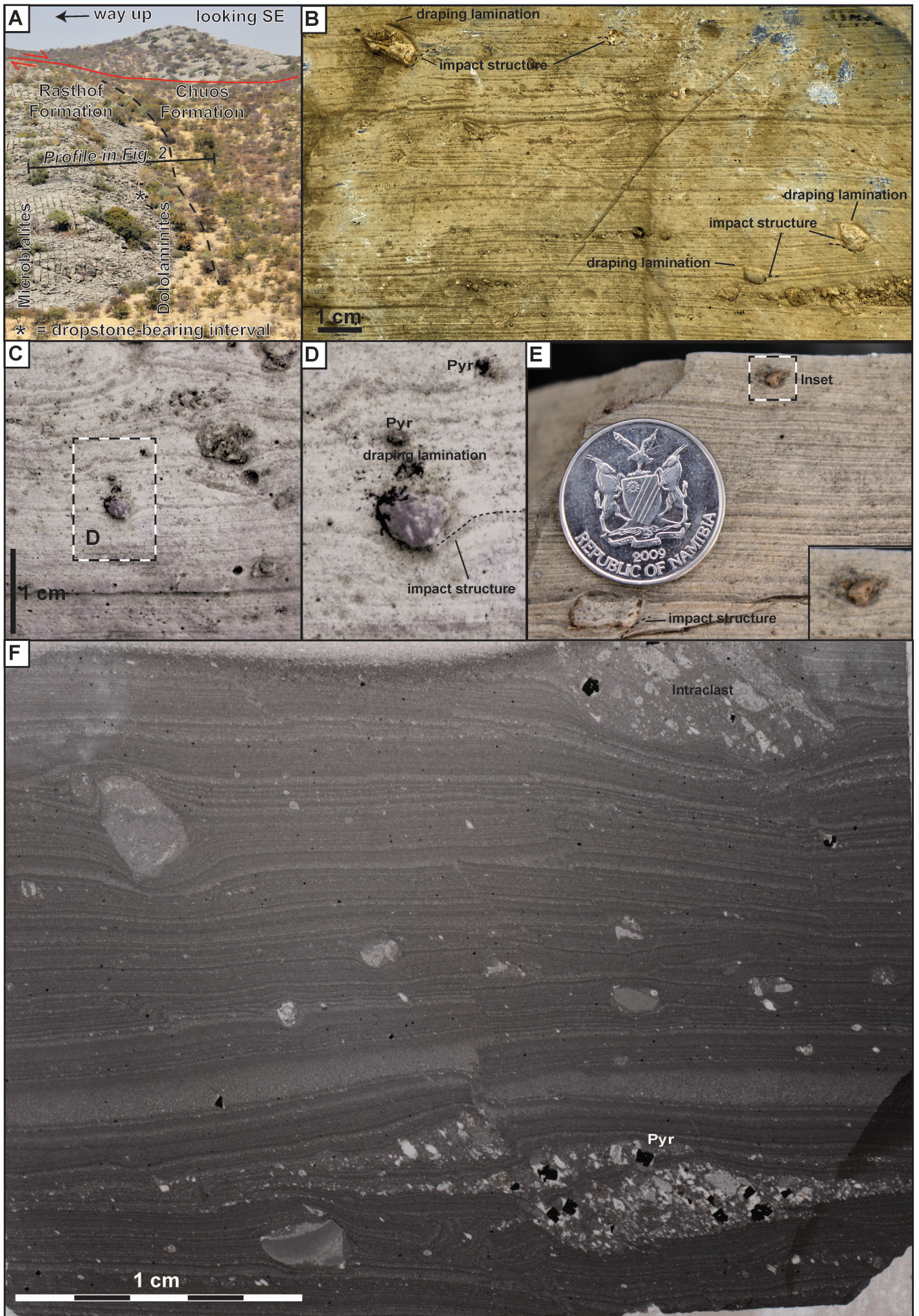


Fig. 4